

**DRYING OF SLICED MATERIALS UNDER THE INFLUENCE OF
ULTRASONIC AND INFRARED RADIATIONS**

by

LOW HUA CHIN

**Thesis submitted in fulfillment of the requirements for the degree of
Master of Science**

JULY 2011

ACKNOWLEDGMENTS

First and foremost, I would like to acknowledge for those have supported and assisted me in my Master of Science program. Thousands of gratitude from me goes to them who dedicated to this project with me.

First of all, my deepest gratitude and appreciation goes to my supervisor, Assoc. Prof. Dr. W.J.N. Fernando who has given me guidance, encouragements, advices and supports during the whole period of this program. I really appreciate for his willingness in spending time with me to accomplish the project and solve the every single problem with me. I also wish to acknowledge my co-supervisor, Prof. Abdul Latif bin Ahmad. The advices and opinions for him really helpful for me to complete the project and they are really appreciated.

Furthermore, I would like to acknowledge the Ministry of Science, Technology and Innovation (MOSTI) for the support extended through an e-Science grant for this project 03-01-05-SF0393. Special thanks to the RCMO of the Universiti Sains Malaysia (USM) for the advice and encouragement given in carrying out the grant during the tenure. Appreciation is also extended to the USM for the award of the USM Fellowship to me in order to carry out the research.

Last but not least, my gratitude to all of my friends and family for supported me and encouraged me in solving problems for this project. Special thanks to my parents, Mr. Low Kee Kong and Mrs. Thye Lian Jin of their encouragement in order to complete this project.

TABLE OF CONTENTS

	Page
Acknowledgements	ii
Table of Contents	iii
List of Tables	ix
List of Figures	xii
List of Plates	xix
List of Abbreviations	xx
List of Symbols	xxi
Abstrak	xxv
Abstract	xxvii

CHAPTER 1 : INTRODUCTION

1.1	Drying Process	1
	1.1.1. Introduction to drying process	1
	1.1.2. Type of drying methods and dryers	2
	1.1.3. Drying of slices	9
	1.1.4. Effective diffusion coefficients	11
1.2	Problem Statement	12
1.3	Scope of Study	13
1.4	Objectives	15
1.5	Organization of Thesis	16

CHAPTER 2 : LITERATURE REVIEW

2.1	Convective Drying	19
2.1.1	Convective drying process	19
2.1.2	Theory of moisture transfer in convective drying	19
2.1.3	Parameters influencing rates in convective drying	20
2.1.3.1	Air velocity	21
2.1.3.2	Air temperature	22
2.1.3.3	Sliced thickness	23
2.2	Diffusion Process in Convective Drying	24
2.2.1	Effective diffusion coefficients	24
2.2.2	Dependence of effective diffusion coefficient on slice thicknesses	29
2.2.3	Analysis of Arrhenius constants and activation energies	30
2.2.3.1	Arrhenius constant	31
2.2.3.2	Activation energy	32
2.2.3.3	Evaluation of Arrhenius constant and activation energy	33
2.3	Enhanced Technologies in Convective Drying	36
2.3.1	Application of ultrasonic energy	36
2.3.1.1	Application and effect of ultrasonic energy	36
2.3.1.2	Previous studies on convective drying rates and effective diffusion coefficients under ultrasonic energy	43
2.3.1.3	Effect of ultrasonic frequency on mechanism of drying and effective diffusion coefficients	46

2.3.2	Infrared radiation	48
2.3.2.1	Application and effect of infrared radiation	48
2.3.2.2	Previous studies on convective drying rates under infrared radiation	52
2.3.2.3	Effect of infrared power on mechanism of drying and effective diffusion coefficients	54
2.3.3	Combined infrared radiation and ultrasonic energy	57
2.3.3.1	Application of combined infrared radiation and ultrasonic energy in drying	57
2.4	Design of Experiment (DOE)	59
2.4.1	Central composite design (CCD)	59
2.4.2	Response Surface Methodology (RSM)	61
2.4.3	Analysis of Variance (ANOVA)	62
2.5	Summary	63

CHAPTER 3 : MATERIALS AND METHODS

3.1	Materials	66
3.1.1	Materials selected	66
3.2	Equipment	68
3.3	Methods	71
3.3.1	Preliminary studies	71
3.3.2	Identification of parameters for study	71
3.3.3	Experimental studies	72
3.3.3.1	Design of Experiment (DOE) study	72
3.3.3.2	Sample preparation	75

3.3.3.3	Drying experiments	75
3.3.3.4	Evaluation of drying rates	76
3.3.3.5	Evaluation of effective diffusion coefficients	76
3.3.3.6	Supplementary experiments	76
3.3.3.7	Experiments of determination of anisotropy of the materials	77
3.3	Modelling Studies	77
3.4	Flow Chart of Project	78

CHAPTER 4 : MODELLING STUDIES

4.1	Theoretical Modelling	81
4.1.1	Model for estimation of effective diffusion coefficients with slice thicknesses	81
4.1.2	Estimation of axial and radial diffusion coefficients, activation energies and Arrhenius constants	86
4.2	Statistical Modelling	86
4.2.1	Analysis of variance (ANOVA) studies of effective diffusion coefficients	86
4.2.2	Analysis of variance (ANOVA) studies of axial and radial diffusion coefficients	87
4.2.3	Analysis of variance (ANOVA) studies of activation energies	87
4.2.4	Analysis of variance (ANOVA) studies of Arrhenius constants	88

CHAPTER 5 : RESULTS AND DISCUSSIONS

5.1	Preliminary Studies	89
5.2	Analysis of Drying Curves	89
5.3	Analysis of Effective Diffusion Coefficients	92
5.3.1	Evaluation of effective diffusion coefficients	92
5.3.2	Statistical analysis of effective diffusion coefficients	96
5.3.2.1	Analysis of Variance (ANOVA) of effective diffusion coefficients	96
5.3.2.2	Response surface plots of effective diffusion coefficients	104
5.4	Theoretical Modelling	114
5.4.1	Study of effective diffusion coefficients with slice thicknesses	114
5.5	Analysis of Axial and Radial Diffusion Coefficients	117
5.5.1	Estimation of axial and radial diffusion coefficients	117
5.5.2	Statistical analysis of axial and radial diffusion coefficients	122
5.5.2.1	Analysis of Variance (ANOVA) of axial and radial diffusion coefficients	128
5.5.2.2	Response surface plots of axial and radial diffusion coefficients	
5.6	Analysis of Arrhenius Constants and Activation Energies	141
5.6.1	Estimation of Arrhenius constants and activation energies	141
5.6.2	Statistical analysis of Arrhenius constants and activation	147

	energies	
5.6.2.1	Analysis of Variance (ANOVA) of Arrhenius constants and activation energies	147
5.6.2.2	Response surface plots of Arrhenius constants and activation energies	158
5.7	Validation of Analysis	163
 CHAPTER 6 : CONCLUSION AND RECOMMEDATION		
6.1	Conclusion	165
6.2	Recommendation	168
 REFERENCES		169
 APPENDICES		
Appendix A	: Drying curve (plot of moisture ratio versus time)	184
Appendix B	: ANOVA of effective diffusion coefficients	193
Appendix C	: Response surface plots of effective diffusion coefficients	199
Appendix D	: Plots of D_{eff} versus value of ℓ^2 for evaluation of axial and radial diffusion coefficient	208
Appendix E	: Plots of $Ln(D_z)$ versus $(1/T)$ and $Ln(D_r)$ versus $(1/T)$ for evaluation of Arrhenius constants and activation energies	211
 LIST OF PUBLICATIONS		217

LIST OF TABLES

	Page
Table 2.1	Slices and thin layer drying models 28
Table 2.2	Evaluated activation energies and Arrhenius constants of the previous works 34
Table 2.3	Types of transducers and their characteristic 37
Table 3.1	Coded and actual values of independent variables for the Design of Experiment (DOE) 72
Table 3.2.	Result from DOE 73
Table 3.3.	Coded and actual values of independent variables for the new DOE 74
Table 3.4.	Result from the new DOE 74
Table 5.1.	Initial moisture content for various types of materials for experimental and from literature 89
Table 5.2.	The evaluated effective diffusion coefficients values for banana slices based on DOE for different slice thicknesses. 93
Table 5.3.	The evaluated effective diffusion coefficients values for cassava slices based on DOE for different slice thicknesses. 94
Table 5.4.	The evaluated effective diffusion coefficients values for pumpkin slices based on DOE for different slice thicknesses 95
Table 5.5.	Analysis of Variance (ANOVA) of effective diffusion coefficients for response surface quadratic model of 0.5×10^{-2} m of banana slices 101
Table 5.6.	Analysis of Variance (ANOVA) of effective diffusion coefficients for response surface quadratic model of 0.5×10^{-2} m of cassava slices 102
Table 5.7.	Analysis of Variance (ANOVA) of effective diffusion coefficients for response surface quadratic model of 0.5×10^{-2} m of pumpkin slices 103
Table 5.8.	The axial diffusion coefficients (D_z) of slices of banana, cassava and pumpkin based on DOE 118

Table 5.9.	The radial diffusion coefficients (D_r) of slices of banana, cassava and pumpkin based on DOE	119
Table 5.10.	Breaking stress for axially and radially cut for slices of banana, cassava and pumpkin respectively	120
Table 5.11.	Analysis of Variance (ANOVA) of axial and radial diffusion coefficients for response surface quadratic model of slices of banana	125
Table 5.12.	Analysis of Variance (ANOVA) of axial and radial diffusion coefficients for response surface quadratic model of slices of cassava	126
Table 5.13.	Analysis of Variance (ANOVA) of axial and radial diffusion coefficients for response surface quadratic model of slices of pumpkin	127
Table 5.14.	The activation energies of axial direction ($E_{a,z}$) based on DOE for slices of banana, cassava and pumpkin	143
Table 5.15.	The activation energies of radial direction ($E_{a,r}$) based on DOE for slices of banana, cassava and pumpkin	144
Table 5.16.	The Arrhenius constants of axial direction ($D_{o,z}$) based on DOE for slices of banana, cassava and pumpkin	145
Table 5.17.	The Arrhenius constants of radial direction ($D_{o,r}$) based on DOE for slices of banana, cassava and pumpkin	146
Table 5.18.	Analysis of Variance (ANOVA) of Arrhenius constants of axial and radial direction for response surface quadratic model of slices of banana	152
Table 5.19.	Analysis of Variance (ANOVA) of Arrhenius constants of axial and radial direction for response surface quadratic model of slices of cassava	153
Table 5.20.	Analysis of Variance (ANOVA) of Arrhenius constants of axial and radial direction for response surface quadratic model of slices of pumpkin	154
Table 5.21.	Analysis of Variance (ANOVA) of activation energies of axial and radial direction for response surface quadratic model of slices of banana	155
Table 5.22.	Analysis of Variance (ANOVA) of activation energies of axial and radial direction for response surface quadratic model of slices of cassava	156
Table 5.23.	Analysis of Variance (ANOVA) of activation energies of axial and radial direction for response surface quadratic	157

model of slices of pumpkin

Table B-1.	Analysis of Variance (ANOVA) of effective diffusion coefficients for response surface quadratic model of 1.0×10^{-2} m of banana slices	193
Table B-2.	Analysis of Variance (ANOVA) of effective diffusion coefficients for response surface quadratic model of 1.0×10^{-2} m of cassava slices	194
Table B-3.	Analysis of Variance (ANOVA) of effective diffusion coefficients for response surface quadratic model of 1.0×10^{-2} m of pumpkin slices	195
Table B-4.	Analysis of Variance (ANOVA) of effective diffusion coefficients for response surface quadratic model of 1.5×10^{-2} m of banana slices	196
Table B-5.	Analysis of Variance (ANOVA) of effective diffusion coefficients for response surface quadratic model of 1.5×10^{-2} m of cassava slices	197
Table B-6.	Analysis of Variance (ANOVA) of effective diffusion coefficients for response surface quadratic model of 1.5×10^{-2} m of pumpkin slices	198

LIST OF FIGURES

	Page
Figure 1.1	Typical drying curve for slices 11
Figure 2.1	Transfer process of the moisture molecules within the solid matrix 32
Figure 2.2	Continuous wave propagation in ultrasonic application 36
Figure 2.3	Behaviour of diffusion flux at (a) convective drying under ultrasound application condition and (b) convective drying conditions. 41
Figure 2.4	Cavitation phenomena 42
Figure 2.5	Electromagnetic Spectrum for infrared region 49
Figure 2.6	Extinction (Reflection, absorption and transmission) of infrared radiation 51
Figure 2.7	The central composite rotatable (CCR), central composite inscribed (CCI) and central composite face centred (CCF) of central composite designs 60
Figure 3.1	Schematic diagram of pilot plant test dryer for ultrasonic and infrared convective drying 70
Figure 3.2	Flow chart of the project 80
Figure 5.1	Response surface plots of effective diffusion coefficient versus air temperature and ultrasonic frequency at three different values of infrared power for 0.5×10^{-2} m slices of banana. 106
Figure 5.2	Response surface plots of effective diffusion coefficient versus air temperature and ultrasonic frequency at three different values of infrared power for 0.5×10^{-2} m slices of cassava 106
Figure 5.3	Response surface plots of effective diffusion coefficient versus air temperature and ultrasonic frequency at three different values of infrared power for 0.5×10^{-2} m slices of pumpkin 107
Figure 5.4	Response surface plots of effective diffusion coefficient versus air temperature and infrared power at three different values of ultrasonic frequency for 0.5×10^{-2} m slices of 109

banana

Figure 5.5	Response surface plots of effective diffusion coefficient versus air temperature and infrared power at three different values of ultrasonic frequency for 0.5×10^{-2} m slices of cassava	109
Figure 5.6	Response surface plots of effective diffusion coefficient versus air temperature and infrared power at three different values of ultrasonic frequency for 0.5×10^{-2} m slices of pumpkin	110
Figure 5.7	Response surface plots of effective diffusion coefficient versus ultrasonic frequency and infrared power at three different values of air temperature for 0.5×10^{-2} m slices of banana	112
Figure 5.8	Response surface plots of effective diffusion coefficient versus ultrasonic frequency and infrared power at three different values of air temperature for 0.5×10^{-2} m slices of cassava	112
Figure 5.9	Response surface plots of effective diffusion coefficient versus ultrasonic frequency and infrared power at three different values of air temperature for 0.5×10^{-2} m slices of pumpkin	113
Figure 5.10	Plot of effective diffusion coefficient (D_{eff}) versus values of t^2 for slices of banana at air temperature of 85°C, 90°C and 95°C	115
Figure 5.11	Plot of effective diffusion coefficient (D_{eff}) versus values of t^2 for slices of cassava at air temperature of 85°C, 90°C and 95°C	115
Figure 5.12	Plot of effective diffusion coefficient (D_{eff}) versus values of t^2 for slices of pumpkin at air temperature of 85°C, 90°C and 95°C	116
Figure 5.13	Response surface plots of axial diffusion coefficient versus air temperature and ultrasonic frequency at three different values of infrared power for slices of banana	130
Figure 5.14	Response surface plots of axial diffusion coefficient versus air temperature and ultrasonic frequency at three different values of infrared power for slices of cassava	130
Figure 5.15	Response surface plots of axial diffusion coefficient versus air temperature and ultrasonic frequency at three different values of infrared power for slices of pumpkin	131

Figure 5.16	Response surface plots of radial diffusion coefficient versus air temperature and ultrasonic frequency at three different values of infrared power for slices of banana	131
Figure 5.17	Response surface plots of radial diffusion coefficient versus air temperature and ultrasonic frequency at three different values of infrared power for slices of cassava	132
Figure 5.18	Response surface plots of radial diffusion coefficient versus air temperature and ultrasonic frequency at three different values of infrared power for slices of pumpkin	132
Figure 5.19	Response surface plots of axial diffusion coefficient versus air temperature and infrared power at three different values of ultrasonic frequency for slices of banana	134
Figure 5.20	Response surface plots of axial diffusion coefficient versus air temperature and infrared power at three different values of ultrasonic frequency for slices of cassava	134
Figure 5.21	Response surface plots of axial diffusion coefficient versus air temperature and infrared power at three different values of ultrasonic frequency for slices of pumpkin	135
Figure 5.22	Response surface plots of radial diffusion coefficient versus air temperature and infrared power at three different values of ultrasonic frequency for slices of banana	135
Figure 5.23	Response surface plots of radial diffusion coefficient versus air temperature and infrared power at three different values of ultrasonic frequency for slices of cassava	136
Figure 5.24	Response surface plots of radial diffusion coefficient versus air temperature and infrared power at three different values of ultrasonic frequency for slices of pumpkin	136
Figure 5.25	Response surface plots of axial diffusion coefficient versus ultrasonic frequency and infrared power at three different values of air temperature for slices of banana	138
Figure 5.26	Response surface plots of axial diffusion coefficient versus ultrasonic frequency and infrared power at three different values of air temperature for slices of cassava	138
Figure 5.27	Response surface plots of axial diffusion coefficient versus ultrasonic frequency and infrared power at three different values of air temperature for slices of pumpkin	139
Figure 5.28	Response surface plots of radial diffusion coefficient versus ultrasonic frequency and infrared power at three different values of air temperature for slices of banana	139

Figure 5.29	Response surface plots of radial diffusion coefficient versus ultrasonic frequency and infrared power at three different values of air temperature for slices of cassava	140
Figure 5.30	Response surface plots of radial diffusion coefficient versus ultrasonic frequency and infrared power at three different values of air temperature for slices of pumpkin	140
Figure 5.31	Response surface plots of Arrhenius constants of axial direction versus ultrasonic frequency and infrared power for slices of banana, cassava and pumpkin respectively	161
Figure 5.32	Response surface plots of Arrhenius constants of radial direction versus ultrasonic frequency and infrared power for slices of banana, cassava and pumpkin respectively	161
Figure 5.33	Response surface plots of activation energies of axial direction versus ultrasonic frequency and infrared power for slices of banana, cassava and pumpkin respectively	162
Figure 5.34	Response surface plots of activation energies of radial direction versus ultrasonic frequency and infrared power for slices of banana, cassava and pumpkin respectively	162
Figure 5.35	Plots of estimated moisture ratio versus experimental moisture ratio for 0.5 cm of slices of banana, cassava and pumpkin respectively	164
Figure 5.36	Plots of estimated moisture ratio versus experimental moisture ratio for 1.5 cm of slices of banana, cassava and pumpkin respectively	164
Figure A-1	Drying curves of each experiment based on DOE in Table 3.2 for 0.5×10^{-2} m of banana slices	184
Figure A-2	Drying curves of each experiment based on DOE in Table 3.2 for 1.0×10^{-2} m of banana slices	185
Figure A-3	Drying curves of each experiment based on DOE in Table 3.2 for 1.5×10^{-2} m of banana slices	186
Figure A-4	Drying curves of each experiment based on DOE in Table 3.2 for 0.5×10^{-2} m of cassava slices	187
Figure A-5	Drying curves of each experiment based on DOE in Table 3.2 for 1.0×10^{-2} m of cassava slices	188
Figure A-6	Drying curves of each experiment based on DOE in Table 3.2 for 1.5×10^{-2} m of cassava slices	189
Figure A-7	Drying curves of each experiment based on DOE in Table 3.2 for 0.5×10^{-2} m of pumpkin slices	190

Figure A-8	Drying curves of each experiment based on DOE in Table 3.2 for 1.0×10^{-2} m of pumpkin slices	191
Figure A-9	Drying curves of each experiment based on DOE in Table 3.2 for 1.5×10^{-2} m of pumpkin slices	192
Figure C-1	Response surface plots of effective diffusion coefficient versus air temperature and ultrasonic frequency at three different values of infrared power for 1.0×10^{-2} m slices of banana	199
Figure C-2	Response surface plots of effective diffusion coefficient versus air temperature and ultrasonic frequency at three different values of infrared power for 1.0×10^{-2} m slices of cassava	199
Figure C-3	Response surface plots of effective diffusion coefficient versus air temperature and ultrasonic frequency at three different values of infrared power for 1.0×10^{-2} m slices of pumpkin	200
Figure C-4	Response surface plots of effective diffusion coefficient versus air temperature and ultrasonic frequency at three different values of infrared power for 1.5×10^{-2} m slices of banana	200
Figure C-5	Response surface plots of effective diffusion coefficient versus air temperature and ultrasonic frequency at three different values of infrared power for 1.5×10^{-2} m slices of cassava	201
Figure C-6	Response surface plots of effective diffusion coefficient versus air temperature and ultrasonic frequency at three different values of infrared power for 1.5×10^{-2} m slices of pumpkin	201
Figure C-7	Response surface plots of effective diffusion coefficient versus air temperature and infrared power at three different values of ultrasonic frequency for 1.0×10^{-2} m slices of banana	202
Figure C-8	Response surface plots of effective diffusion coefficient versus air temperature and infrared power at three different values of ultrasonic frequency for 1.0×10^{-2} m slices of cassava	202
Figure C-9	Response surface plots of effective diffusion coefficient versus air temperature and infrared power at three different values of ultrasonic frequency for 1.0×10^{-2} m slices of pumpkin	203

Figure C-10	Response surface plots of effective diffusion coefficient versus air temperature and infrared power at three different values of ultrasonic frequency for 1.5×10^{-2} m slices of banana	203
Figure C-11	Response surface plots of effective diffusion coefficient versus air temperature and infrared power at three different values of ultrasonic frequency for 1.5×10^{-2} m slices of cassava	204
Figure C-12	Response surface plots of effective diffusion coefficient versus air temperature and infrared power at three different values of ultrasonic frequency for 1.5×10^{-2} m slices of pumpkin	204
Figure C-13	Response surface plots of effective diffusion coefficient versus ultrasonic frequency and infrared power at three different values of air temperature for 1.0×10^{-2} m slices of banana	205
Figure C-14	Response surface plots of effective diffusion coefficient versus ultrasonic frequency and infrared power at three different values of air temperature for 1.0×10^{-2} m slices of cassava	205
Figure C-15	Response surface plots of effective diffusion coefficient versus ultrasonic frequency and infrared power at three different values of air temperature for 1.0×10^{-2} m slices of pumpkin	206
Figure C-16	Response surface plots of effective diffusion coefficient versus ultrasonic frequency and infrared power at three different values of air temperature for 1.5×10^{-2} m slices of banana	206
Figure C-17	Response surface plots of effective diffusion coefficient versus ultrasonic frequency and infrared power at three different values of air temperature for 1.5×10^{-2} m slices of cassava	207
Figure C-18	Response surface plots of effective diffusion coefficient versus ultrasonic frequency and infrared power at three different values of air temperature for 1.5×10^{-2} m slices of pumpkin	207
Figure D-1	Plot of effective diffusion coefficient versus values of ℓ^2 for slices of banana for each experiment based on DOE in Table 3.2	208
Figure D-2	Plot of effective diffusion coefficient versus values of ℓ^2 for slices of cassava for each experiment based on DOE in	209

Table 3.2

Figure D-3	Plot of effective diffusion coefficient versus values of ℓ^2 for slices of pumpkin for each experiment based on DOE in Table 3.2	210
Figure E-1	Plots of $\ln(D_z)$ versus $(1/T)$ for slices of banana for each experiment based on DOE in Table 3.4	211
Figure E-2	Plots of $\ln(D_r)$ versus $(1/T)$ of for slices of banana for each experiment based on DOE in Table 3.4	212
Figure E-3	Plots of $\ln(D_z)$ versus $(1/T)$ for slices of cassava for each experiment based on DOE in Table 3.4	213
Figure E-4	Plots of $\ln(D_r)$ versus $(1/T)$ for slices of cassava for each experiment based on DOE in Table 3.4	214
Figure E-5	Plots of $\ln(D_z)$ versus $(1/T)$ for slices of pumpkin for each experiment based on DOE in Table 3.4	215
Figure E-6	Plots of $\ln(D_r)$ versus $(1/T)$ for slices of pumpkin for each experiment based on DOE in Table 3.4	216

LIST OF PLATES

	Page
Plate 3.1 Photograph of the pilot plant test dryer	70
Plate 5.1 Different direction of cutting: (a) perpendicular cut and (b) parallel of the slices of banana	121
Plate 5.2 Different direction of cutting: (a) perpendicular cut and (b) parallel of the slices of cassava	121
Plate 5.3 Different direction of cutting: (a) perpendicular cut and (b) parallel of the slices of pumpkin	121

LIST OF ABBREVIATION

$adj-R^2$	Adjusted correlation coefficient
ANOVA	Analysis of Variance
CCD	Central composite design
CCI	Central composite inscribed
CCF	Central composite face centred
CCR	Central composite rotatable
CV	Coefficient of variation
DOE	Design of Experiment
F-test	Fisher's statistical test
F -value	Fisher variance ratio
$pred-R^2$	Correlation coefficient for predicted model
$PRESS$	Predicted residual sum of squares
RF	Radio frequency
RSM	Response surface methodology

LIST OF SYMBOLS

Symbols	Description	Unit
A	surface area of material	m^2
A	constant for slice and thin layer models	-
a_v	average radius of the cylindrical slice	m
B	constant for slice and thin layer models	-
C	constant for slice and thin layer models	-
C	moisture concentration	kg water/ m^3 dry sample
C_o	initial moisture concentration	kg water/ m^3 dry sample
C_e	equilibrium moisture concentration	kg water/ m^3 dry sample
C^*	moisture concentration ratio, given by $(C - C_e)/(C_o - C_e)$	-
C	sound velocity	m/s
c_o	speed of light	km/s
D_{eff}	effective diffusion coefficient	m^2/s
D_o	Arrhenius constant	m^2/s
D_r	lateral or radial diffusion coefficient	m^2/s
D_z	longitudinal or axial diffusion coefficient	m^2/s
$E_b(T)$	total power radiated	W
$E_{b, \lambda}(T, \lambda)$	spectra blackbody emissive power distribution	
E	energy density	N/m^2
E_a	activation energy	kJ/mol
f	frequency of ultrasonic	Hz
H_λ	transmitted spectral irradiance	$W/m^2 \cdot \mu m$
$H_{\lambda o}$	incident spectral irradiance	$W/m^2 \cdot \mu m$
h	Planck's constant	J·s

I	intensity of ultrasonic energy	W/cm^2
$J_0(x)$	Bessel function of zero order	-
j	factors of observations	-
k	constant slice and for thin layer models	-
k_c	moisture transfer coefficient	$\text{kg w/m}^2/\text{s}$
k_o	constant for slice and thin layer models	-
k_l	constant for slice and thin layer models	-
L	jump length	m
ℓ	thickness of samples	m
$M(t)$	moisture content at time, t	kg water/kg dry sample
$M(0)$	initial moisture content at $t=0$	kg water/kg dry sample
$M(\infty)$	equilibrium moisture content at $t \rightarrow \infty$	kg water/kg dry sample
$M_R(t)$	moisture ratio at time, t	-
n	constant for thin layer models	-
P	applied electric power of sonicator	dB
P_a	pressure amplitude	dB
$P_{a,max}$	maximum pressure amplitude	dB
$p(x,t)$	ultrasonic pressure at position, x and time, t	-
p_{op}	ultrasonic pressure for the positive (x) directed components	-
p_{on}	ultrasonic pressure for the negative ($-x$) directed components	-
Q_{st}	isosteric heat	kJ/mol
R	constant for Arrhenius relation	$\text{kJ/mol}\cdot\text{K}$
R_c	drying rate	$\text{kg H}_2\text{O/s}$
R^2	correlation coefficient	-
r	radial distance from the central axis of	m

the slice

S_d	entropy	kJ/mol
T	air temperature	K
t	drying time	s
u	mass of absorbing medium per unit area	kg/m ²
$u(x, t)$	particle velocity at position, x and time, t	-
u_{op}	particle velocity amplitudes for the positive (x) directed components	-
u_{on}	particle velocity amplitudes for the negative ($-x$) directed components	-
V	effective vibrational frequency of the moisture molecules	Hz
v	air velocity	m/s
x	position of moisture diffuse from one point to another point	m
x_i	independent variable	
$W(x, t)$	moisture content at position x and time t	kg water
W_o	initial weight of sample	kg
W_f	final weight of samples	kg water
y_i	dependent variable	-
z	distance of a point within slice along the axis of cylindrical slice from the bottom of slice	m

Greek symbols

α	distance of axial points in the design	-
α_o	mean of the observations	-
α_j	unknown constant	-
ϕ	lag phase for ultrasonic wave equation	-
ϕ_{air}	air relative humidity of the air at	-

equilibrium with the surface of the material

ϕ_e	relative humidity of the hot air	-
π	pi (3.14159265....)	-
λ	wavelength of ultrasonic	nm
λ_{\max}	peak wavelength of infrared radiation	μm
ρ	density of material	-
ρ_{ds}	dry solid density	kg/m^3
σ	Stefan–boltzmann constant	$\text{W/m}^2\text{k}^4$
σ^2	Variance	-
σ_λ^*	spectral extinction coefficient	m^2/kg
ε_l	independent random variables at $n=1$	-
ε_n	independent random variables at n	-

Pengeringan bahan hirisan di bawah pengaruh Sinaran Ultrasonik dan Inframerah

ABSTRAK

Pengeringan olakan biasanya digunakan dalam pengawetan produk pertanian. Kadar pengeringan secara umumnya bergantung kepada pekali resapan kelembapan berkesan dalam bahan-bahan. Penambahan kuasa dan frekuensi ultrasonik dan inframerah telah diketahui boleh meningkatkan kadar proses pengeringan olakan. Objektif utama bagi kajian ini adalah untuk mengkaji pengaruh frekuensi ultrasonik dan kuasa inframerah kepada pekali resapan berkesan bagi kelembapan dalam bahan-bahan. Eksperimen telah dijalankan untuk pisang, ubi kayu dan labu berdasarkan Rekabentuk Eksperimen dalam julat suhu udara (85°C , 90°C dan 95°C) dengan frekuensi ultrasonik (0 kHz, 20 kHz and 50 kHz) dan kuasa inframerah (0 W/m^2 , 757.50 W/m^2 and 1515 W/m^2). Data terkumpul daripada eksperimen telah dimasukkan ke dalam persamaan untuk mendapatkan pekali resapan berkesan. Pekali resapan berkesan dianalisis dengan statistik oleh Analisis Varians dengan parameter frekuensi ultrasonik dan kuasa inframerah bagi setiap ketebalan hirisan. Pekali resapan berkesan diperhatikan bertambah dengan penambahan frekuensi ultrasonik dan kuasa inframerah.

Pekali resapan berkesan juga diperhatikan sangat bergantung kepada ketebalan hirisan. Pergantungan pekali resapan berkesan kepada ketebalan hirisan juga telah dikaji. Satu model teori telah dibina untuk menghubungkaitkan pekali resapan kelembapan berkesan dalam bahan-bahan dengan ketebalan hirisan, pekali resapan

paksi dan jejarian. Model itu didapati menunjukkan kelainan pekali resapan berkesan dengan ketebalan hirisan secara baik dan ia disahkan dengan data eksperimen bagi pekali korelasi yang 0.948 ke 0.999 bagi bahan-bahan terpilih. Nilai pekali resapan paksi didapati lebih tinggi daripada pekali resapan jejarian disebabkan oleh sifat bahan-bahan yang tak isotropi. Pekali resapan paksi dan jejarian dianalisis dengan statistik oleh Analisis Varians dengan parameter suhu udara, frekuensi ultrasonik dan kuasa inframerah. Pekali resapan paksi dan jejarian juga diperhatikan bertambah dengan penambahan suhu udara, frekuensi ultrasonik dan kuasa inframerah.

Penilaian bagi tenaga pengaktifan dan pemalar Arrhenius telah diperolehi daripada persamaan Arrhenius. Analisis statistik (Analisis Varians) untuk tenaga pengaktifan dan pemalar Arrhenius dengan frekuensi ultrasonik dan kuasa inframerah telah dijalankan. Didapati tenaga pengaktifan berkurang dengan penambahan frekuensi ultrasonik dan kuasa inframerah tetapi pemalar Arrhenius bertambah dengan penambahan frekuensi ultrasonik dan kuasa inframerah. Sebab-sebab untuk sifat ini telah dikaji. Bagi semua pekali resapan berkesan, paksi dan jejarian, tenaga pengaktifan dan pemalar Arrhenius diperhatikan adalah dikuasai terutamanya kuasa inframerah, suhu udara dan frekuensi ultrasonik.

Drying of Slice Materials under the Influence of Ultrasonic and Infrared Radiations

ABSTRACT

Convective drying has been commonly used in preservation of the agricultural products. The respective drying rates generally depend on the effective diffusion coefficients of moisture within the materials. Increase in ultrasonic power and frequency as well as infrared power have been found to enhance the convective drying process rates. The main aim of this work is to study the influence of the ultrasonic frequency and infrared power on the effective diffusion coefficients of moisture within the materials. For this purpose, experiments were carried out for banana, cassava and pumpkin based on the Design of Experiment (DOE) in the ranges of three air temperatures (85°C, 90°C and 95°C) with ultrasonic frequencies (0 kHz, 20 kHz and 50 kHz) and with infrared power (0 W/m², 757.50 W/m² and 1515 W/m²). The data collected from experiments were employed to determine the effective diffusion coefficients. The effective diffusion coefficients were statistically analyzed by Analysis of Variance (ANOVA) with parameters ultrasonic frequencies and infrared power for each slice thickness. The effective diffusion coefficients were observed to increase with increasing of ultrasonic frequencies and infrared power.

The effective diffusion coefficients were also observed strongly dependent on slice thickness. The dependence of the effective diffusion coefficients on the slice thickness was studied thereafter. A theoretical model was developed in order to correlate effective diffusion coefficient of moisture within the materials with slice

thickness as well as axial and radial diffusion coefficients. The model was found to describe the variation of effective diffusion coefficient with slice thickness very satisfactorily and it was validated with the experimental data with correlation coefficient of 0.948 to 0.999 for selected materials. The values of axial diffusion coefficients were found to be higher than radial diffusion coefficients due to anisotropic behaviour of the materials. The axial and radial diffusion coefficients were analyzed with the statistical analysis (ANOVA) with air temperatures, ultrasonic frequency and infrared power. The axial and radial diffusion coefficients too were observed to increase with increasing of air temperatures, ultrasonic frequencies and infrared power.

The evaluation of the activation energies and Arrhenius constants were carried out by Arrhenius equation. Statistical analysis (ANOVA) of activation energies and Arrhenius constants were carried out with ultrasonic frequency and infrared power. The activation energies were observed to decrease with increasing of ultrasonic frequency and infrared power but Arrhenius constants were observed to increase with increasing of ultrasonic frequency and infrared power. Reasons for this behaviour are examined. All the effective, axial and radial coefficients of diffusion, the Arrhenius constants and the activation energies were observed to be controlled primarily by the infrared power, next by the temperature of drying and thereafter by ultrasonic frequency.

CHAPTER 1

INTRODUCTION

1.1 Drying Process

1.1.1 Introduction to drying process

Drying process is described as a unit operation which converts wet porous material or a slurry into a solid product of significantly low moisture content (Noomhorm, 2007). It is a complex process involving mass transfer and heat transfer. Drying processes and equipments have been categorized according to the nature of material, the method of heat supply and the method of operation (Treybal, 1980; Strumillo and Kudra, 1986).

In drying of most materials, particularly in the food industries, microorganisms exist at higher moisture levels (Earle, 1983). These microorganisms generally are promoted undesired changes in the chemical composition of the food with presence of the water especially quality of food. This process caused the food decay and spoilage. The microorganisms are found unable to grow and multiply in the absence of sufficient water (Earle, 1983). The reactions related to decay are greatly minimized by drying in the absence of water since the microorganism's enzymes cannot function in the absence of water.

Apart from preservation of the quality of the agricultural products, drying also provided lighter weight for transportation, better return for the farmer and less space for storage (Noomhorm, 2007). Therefore, drying process has become essential and significant process for the food industry in order to preserve food quality and stability with light weight of products for convenient of transportation for marketing.

1.1.2 Type of drying methods and dryers

Drying technology has evolved from the simple of solar drying to current technologies, such as convective tray drying, spray drying, fluidized bed drying, belt conveyor drying, pneumatic conveyor drying, rotary drying, tunnel drying, drum drying, kiln drying, tower drying, vacuum drying, freeze drying and novel drying technologies such as microwaves drying, osmotic drying, infrared radiations drying, acoustic drying such as ultrasonic, radio frequency (*RF*). These drying technologies have been divided into four generations:

a) First generation of dryers

Cabinet and bed type dryers (convective tray, belt, rotary, tunnel, kiln, tower,) fall into first generation. These dryers involve hot air flowing over the surface of the product to remove water from the surface (Barbosa-Canovas and Vega-Mercado, 1996). The dryers within this category are mostly suitable for solid materials such as sliced fruits and vegetables, grains or chunked products and they are mostly available in food industries.

Convective drying has been one of the most widely used methods for drying process. It is a simultaneous heat transfer and mass transfer process with hot air flowed over the materials and removed the moisture on the surface of the materials due to convection effects (Noomhorm, 2007). The hot air also has provided the energy for moisture removal within the materials. Several researchers were carried out the studies on convective drying process of agricultural products such as potato (Desmorieux and Decaen, 2005), spirulina (Hassani *et al.*, 2007), onion flakes

(Kumar and Tiwari, 2007), potato and carrot (Srikiatden and Roberts, 2008) and mango (Barati and Esfahani, 2010).

The tray dryer is one of the common equipments for the convective drying. It is made of trays held in a cabinet and is connected to a source of air heated by electrically, by gas, diesel, bio-mass such as rice husk or solar. The hot air is flowed over the samples in the chamber of the dryer which is promoted evaporation of moisture on the surface of the sample (Noomhorm, 2007). The air temperature is usually controlled by a thermostat and normally set between 50°C to 100°C. The air enters the chamber containing the trays, then flows through the trays and exits from an opening of the chamber. Hot air entering a dryer usually contains low relative humidity leading to high driving force for drying process and thus removes the moisture of the product efficiently. The rate of moisture removal (drying) for this process is dependent on the conditions of the air, the properties of the sample and the design of the dryer (Earle *et al.*, 2004). Higher temperature speeds up diffusion of moisture inside the materials and the drying process is rapid but resulting in surface hardening of the products. Tray dryers are the most suitable equipment in terms of cost and output for small as well medium scale of drying process.

b) Second generation of dryers

The second-generation dryers are used for drying the slurries and pastes. The fluidized bed dryer, pneumatic dryer, spray dryers and drum dryers fall into this category for powders and flakes as final products. Thus, these dryers are applicable for the drying of the sample in form of slurries and pastes rather in solid form of agricultural products.

In fluidized bed drying, heat is supplied by the fluidization gas and heating surfaces such as panels or tubes in fluidized bed dryer (GEA Barr-Rosin, 2011). The air is supplied and flows through the bed of solids at a velocity sufficient to support the weight of particles in a fluidized state. A very high heat and mass transfer are obtained as a result of the intimate contact with the solids and the differential velocities between individual particles and the fluidizing gas (GEA Barr-Rosin, 2011). The fluidized bed drying has been used to dry products in food, chemical, mineral and polymer industries and the range of feed materials are powders, crystals and granules (GEA Barr-Rosin, 2011). The advantages of fluidized bed drying are easy material transport, high rates of heat exchange at high thermal efficiency and preventing overheating of individual particles.

In pneumatic drying, wet material is dispersed into the heated air or gas (GEA Barr-Rosin, 2011). The material dries using the heat as it is conveyed and the product is separated using cyclones or bag filters. Pneumatic dryers have been used to dry products in many industries including food, chemical, mineral and polymer (GEA Barr-Rosin, 2011). A broad range of feed materials including powders, cakes, granules, flakes, pastes, gels and slurries can be processed.

Spray drying is a special drying method and it is involved particle formation and drying processes simultaneously. The feed is transformed from a fluid state into droplets and then into dried particles by spraying a hot drying medium into the bulk spray continuously (Masters, 1991). Spray drying has a lot of advantages if compared with the first generation dryers of fluidized bed drying. The main differences between spray drying and fluidized bed drying are the feed characteristics

(in fluid state for spray drying), residence time (5 s to 100 s for spray drying and 1 minutes to 300 minutes for fluidized bed drying) and particle size (10 μm to 500 μm for spray drying and 10 μm to 3000 μm for fluidized bed drying). The advantages of spray drying (Masters, 1991) are continuous, easy and controllable drying process, the powder properties remain constant throughout the dryer when drying conditions are constant and applicable to heat-sensitive and heat-resistant materials.

Drum dryers is employed an indirect heat transfer drying process through the surface of material and produce powdered and flaked products. These products are widely used in bakery goods, cereal, granola, beverages and dairy foods. It consists of hollow metal cylinders that rotate on horizontal axes and heated internally by steam, hot water or other heating medium (R. Simon (Dryers) Ltd., 1900). The important aspects to be considered for a drum dryer are uniform thickness of the film on the drum surface, speed of rotation and heating temperature. The advantages of drum drying are high drying rates and energy efficiency (R. Simon (Dryers) Ltd., 1900).

c) Third generation of dryers

In the third generation of dryers, these dryers apply the concept of change in physical properties of materials such as low vapour pressure and osmotic effect in order to improve drying process. Freeze drying and osmotic drying fall into third generation of drying methods. Freeze drying is used to overcome structural damages and improve the quality of the products in form of aroma and flavour (Karel, 1975; Dalgleish, 1990). Osmotic drying is used for fruits and vegetables processing

by immersion in a hypertonic solution (sugar, salt or glycerol) (Raoult-Wack *et al.*, 1989).

Freeze drying process consists of two steps where the product is frozen and dried by direct sublimation under reduced pressure (Vega-Mercado *et al.*, 2001). The first step of freezing process is very rapid process to obtain a product with small ice crystals and in an amorphous state. The second step of drying process is involved lowering the pressure to allow ice sublimation. Three important design variables for this process are vacuum inside the chamber, radiant energy flux applied to the sample and temperature of the condenser. The main advantages of the freeze drying are low processing temperature and absence of air thus preventing decay. The drying process temperature is lower than ambient temperature for minimization of product damage compared with products for high temperature of drying process usually undergo changes in structure, texture, appearance and flavour (Longmore, 1971).

Osmotic drying is the drying process of immersion of sample in a hypertonic solution (sugar, salt, sorbitol or glycerol) (Raoult-Wack *et al.*, 1989). The osmotic drying system consists mainly of a storage tank with the osmotic solution, followed by a pump to control the flow rate at the processing tank. The sample is placed in the processing tank and the osmotic solution is pumped in at a constant rate. Osmotic drying process is involved the simultaneous flow of water and solutes (Garcia *et al.*, 2007). Water and food solutes were diffused from the food to the concentrated solution and solution solutes from the osmotic solution were diffused into the food. But the solution solute transfer is limited due to differential

permeability of cellular membranes. Thus, more water is transferred rather than solution solute is transferred for this process.

d) Fourth generation of dryers

This generation of dryers is the latest, innovative and advanced drying technologies including microwaves, radio frequency, ultrasonic, infrared and etc. Each of these technologies has a specific application based on the final quality attributes of the products and the physical or chemical characteristics of the samples. Thus, new approach in enhancement of moisture diffusivity is affected by introduction of the technologies of this generation of dryers.

Microwave drying takes advantage of the polarization that takes place at molecular and atomic levels when microwaves are applied on wet materials to be dried. The molecules within the material generally are aligned with the changing electric field, the heat is developed in a material by an alternating electromagnetic field from the polarization process within the product (Vega-Mercado *et al.*, 2001). The arrangement of atoms in a water molecule makes it polar and making them easily heated using microwave energies. Similar to microwaves, radio frequency too uses electromagnetic energy to heat products. The benefits of radio frequency are higher than the benefits of microwave with higher level of heating and processing speed, better product quality and yields due to uniform and self-limiting drying process, amenable to automation and process control as well as higher energy efficiencies (PSC-Power Systems, 1999).

Ultrasonic energy has been an application of innovative acoustic energy for assisting of the process rates. It has been used in food industry such as separation process of an emulsion into its component aqueous and oil phases, crystallization process to control the size and rate of development of ice crystals in frozen foods, fermentation process of sake, beer and wine, extraction process of organic compound from plants or seeds (Rodrigues and Fernandes, 2008). It has also been applied in the drying process. Ultrasonic has been found to improve the drying process in terms of time of drying and quality of the final products. Ultrasonic energy has been studied for the drying process for the agricultural products including pre-treatment in the drying process (Fernandes *et al.*, 2008), osmotic drying (Fernandes *et al.*, 2009) and force air or air borne drying process (Sarabia *et al.*, 2002).

Over the past several years, infrared radiations have been widely used in the electronics fields but less predominantly applied in the food processing industry (Krishnamurthy *et al.*, 2008). However, many studies have been made with drying process with infrared radiation of foods in the last few years. This is due to many advantages of drying process with infrared application. Several researchers have studied the drying process with infrared radiations such as potato (Afzal and Abe, 2004), various vegetables (Hebbar *et al.*, 2004), banana (Nowak and Lewicki, 2004), onion (Pathare and Sharma, 2006) and apple (Zhongli *et al.*, 2008). The advantages of applying infrared to drying process include versatility, simplicity of equipment, fast response of drying process, easy installation to any drying chamber and low capital cost (Sun *et al.*, 2007). Infrared radiation also gives the advantages of shorter drying time, high energy efficient, high quality products, uniform temperature in the

product and reduced air flow across the product (Sharma *et al.*, 2005a). The applications of ultrasonic and infrared in drying processes are discussed in detail in later chapter of this thesis.

Combination of infrared radiation and ultrasonic energy gives the advantages from both infrared radiation and ultrasonic energy which are fourth generation techniques. These techniques have been applied with convective drying practices which have improved the drying process with high efficiency. Such combination gives the opportunity to improve drying process with lower energy usage compared with traditional thereby results in reduction of greenhouse gases.

1.1.3 Drying of slices

As described earlier, drying process is used to dry the materials including particles, solid materials such as slices of fruits and vegetables, slurries and pastes by using different mechanisms such as convection (convective drying), direct heating (drum dryer), spray drying, fluidized bed drying and pneumatic drying with or without ultrasonic and/or infrared application. However, the above application in agricultural sector related to fruits and vegetables are limited to convective drying. In the agricultural sector, dried fruits and vegetables are in high and noticeably increasing in demand in the market. They have high commercial value demanded by the gastronomic businesses including dessert, ice cream, cocktails, salads and sweet cuisine (Lemus-Mondaca *et al.*, 2008). This is due to their aroma, colour and flavour characteristics can be preserved by controlled the drying process. Drying of slices of fruits and vegetables are commonly in agricultural industries for easy of preservation, packing, transport and storage. The drying process commonly has been carried out

by previous researchers using the sliced materials such as banana (Johnson *et al.*, 1998; Nguyen and Price, 2007), grape leather (Aysun *et al.*, 2002) and wheat-flour yogurt (Senol and Medeni, 2002). The slice thickness of the materials has been observed to influence the drying process (Aysun *et al.*, 2002; Mwithiga and Olwal, 2005; Rao *et al.*, 2007; Doymaz and Gol, 2009).

A standard drying curve for convective drying of slices is similar to other shapes of materials and has been observed to consist of three stages including preheating, constant-rate and falling-rate stage as shown in Figure 1.1 (Hui and Welti-Chanes, 2008). Preheating stage (AB) is the equilibrium stage where the materials are heated to the drying temperature. In constant-rate period (BC), the moisture is evaporated from the saturated surface of materials with the decreasing proportional rate of the moisture content of the materials. At this stage, the temperature is generally constant and approaching the bulk temperature of air. The falling-rate period (CD) occurs after critical moisture content (X_c) of the material is reached. The resistance for transfer of moisture from the internal porous to the surface of the materials thereafter increases leading to a different pattern (DE) which could still be regarded as a falling rate. Most of the agricultural products are reported to be under falling rate period (Swami *et al.*, 2007; Doymaz, 2007; Doymaz and Gol, 2009; Sojak and Glowacki, 2010).

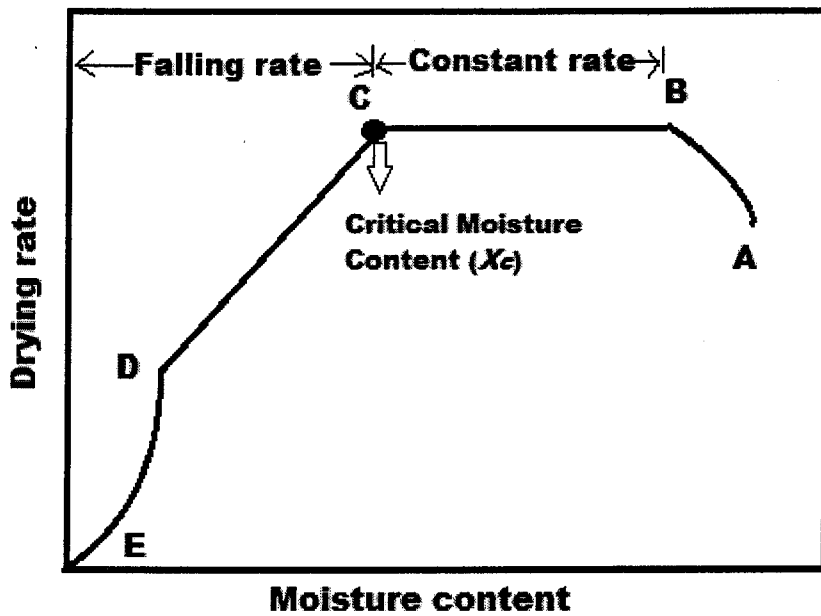


Figure 1.1. Typical drying curve for slices.

1.1.4 Effective diffusion Coefficients

Moisture diffusion from the interior of the solid to the outer surface of a slice is observed to be an important factor in the convective drying process. The moisture reaching the surface of material after such diffusion, evaporates and arriving into the air due to convection (Puyate and Lawrence, 2006). Combination of several other transport mechanisms including capillary flow, liquid diffusion, vapour diffusion, viscous flow could also govern such moisture movement (Valentas *et al.*, 1997). However, diffusion is generally accepted as the principal mechanism of moisture transport in drying processes (Jorge *et al.*, 2002; Togrul and Pehlivan, 2003; Gavrila *et al.*, 2008). Moisture diffusivity in materials such as in starch can strongly be affected by the physical structure particularly the bulk porosity of the material. Moisture diffusivity of food materials such as fruits and vegetables has been estimated by the analysis of drying rates. Thus, drying process is observed to be governed by the diffusion coefficients of moisture. By enhancing the diffusion

coefficients, the drying rates of the process have been enhanced (Johnson *et al.*, 1998; Aysun *et al.*, 2002; Senol and Medeni, 2002; Nguyen and Price, 2007; Bains and Langrish, 2008). Even though the drying rates have been observed to be enhanced by utilization of fourth generation techniques such as ultrasonic and infrared applications, only very little effort has been reported to study the theoretical aspects of convective drying with combined ultrasonic and infrared applications and the relevant diffusion coefficients.

1.2 Problem Statement

Drying is the most common process for the preservation of the agricultural products for reduction of the moisture inside the agricultural products to prevent the microbial spoilage and aging toward them (Noomhorm, 2007). In addition, drying process also give the advantages of lighter weight and minimum space for storage, packing and transportation for marketing purpose. Therefore, this process is appropriate way for preservation of food without adding any chemicals. Nevertheless, the disadvantages of convective drying are lengthy time and low energy efficiency resulting in expensive of the process during the falling rate period (Zhongli *et al.*, 2008). Thus, the techniques of infrared radiation and ultrasonic energy can be integrated into the convective drying in order to enhance the efficiency of the process by giving the better energy efficiency, lower of the environment impact and produce better quality products at lower costs (Kudra and Mujumdar, 2009). This method has been improved the energy efficiency by greatly minimizing the drying time (Valentino *et al.*, 2002; Brncic *et al.*, 2010).

The drying rate is dependent on effective diffusion coefficient of moisture. The efficient drying process could be approached by enhancing the effective diffusion coefficient of moisture. The effective diffusion coefficient of moisture could be enhanced by integrating ultrasonic energy and infrared radiation into traditional convective drying. Several studies has proven that ultrasonic energy (Carcel *et al.*, 2007a; García-Pérez *et al.*, 2007; Azoubel *et al.*, 2009; García-Pérez *et al.*, 2009; Ortuno *et al.*, 2010) and infrared radiation (Sharma *et al.*, 2005; Pathare and Sharma, 2006; Das *et al.*, 2009; Nuthong *et al.*, 2010) have affected to the moisture diffusivity and thus has affected to the energy efficiency. However, research on combined convective drying process with infrared radiation and ultrasonic energy is very limited.

This research mainly aims to study the effective diffusion coefficients with combined infrared and ultrasonic radiations. In this study, the advantages of the combined infrared and ultrasonic radiations with convective drying have been approached.

1.3 Scope of Study

Study of effective diffusion coefficients is a very important aspect in the drying research because drying rates depend on the effective diffusion coefficients. Effective diffusion coefficients are dependent on the different materials based on different structure within the materials in addition to other parameters such as thicknesses of sliced materials (Tutunzu and Labuza, 1996; Johnson *et al.*, 1998; Aysun *et al.*, 2002; Senol and Medeni, 2002; Nguyen and Price, 2007) and air temperature (Karim and Hawlader, 2005; Doymaz, 2007; Nguyen and Price, 2007;

Corzo *et al.*, 2008). Three materials have been selected in this study based on their structure namely banana (a sticky materials), cassava (a material with a longitudinal fibrous structure) and pumpkin (a gourd type of materials).

A tray dryer integrated with infrared lamp and sonicator or ultrasonic generator was set up for experiments. Preliminary studies were carried out to determine the initial moisture content of each selected materials. Parameters namely ultrasonic frequency, infrared power, air temperature and slice thickness were identified for drying experiments. The slice thicknesses, air temperatures, infrared power and ultrasonic frequencies selected were 0.5×10^{-2} m to 1.5×10^{-2} m, 85°C to 95°C , 0 W/m^2 to 1515 W/m^2 and 0 kHz to 50 kHz respectively. Twenty set of combination of parameters of air temperature, ultrasonic frequency and infrared power based on Design of Experiment (DOE) were selected and experiments were carried out for each material experimented. Several supplementary experiments were also carried out for the verification of the model developed thereafter. The data collected from experiments were employed in order to evaluate the drying rates and effective diffusion coefficients.

Modelling studies were carried out in order to correlate the effective diffusion coefficients with respective parameters. It consisted of two sections namely theoretical modelling and statistical modelling. In theoretical modelling, a mathematical model was formulated for studying the dependence of effective diffusion coefficients on slice thicknesses. The axial and radial diffusion coefficients were evaluated from the model formulated which showed anisotropy of materials. An experiment was carried out in order to verify the anisotropic behaviour of the

materials. Activation energies and Arrhenius constant were evaluated from the Arrhenius relation thereafter. The effective diffusion coefficients were analysed with air temperature, ultrasonic frequency and infrared power at a given slice thickness by Analysis of Variance (ANOVA). The ANOVA studies of variation of axial and radial diffusion coefficients with air temperature, ultrasonic frequency and infrared power were analyzed. ANOVA of activation energies and Arrhenius constant were carried out with ultrasonic frequency and infrared power and analysed.

The estimated axial and radial diffusion coefficients were used to regenerate moisture ratio at an intermediate point of drying process. The estimated values were compared with the experimental data and showed the excellent fit.

1.4 Objectives

The main objective of this study is to evaluate the dependence of the effective diffusion coefficients on the ultrasonic frequency and infrared power. For this purpose, the following itemised objectives are presented as:

1. To carry out experimental studies of drying of slices of banana, cassava and pumpkin under air temperatures (85°C to 95°C), ultrasonic frequencies (0 kHz to 50 kHz) and infrared powers (0 W/m² to 1515 W/m²) at a given slice thicknesses (0.5×10^{-2} m to 1.5×10^{-2} m) based on Design of Experiment (DOE).
2. To analyse the data drying curves obtained in order to evaluate the effective, axial and radial diffusion coefficients as well as activation energies and Arrhenius constants of moisture for the three selected materials.

3. To statistical analyse the effective, axial and radial diffusion coefficients as well as activation energies and Arrhenius constants evaluated with Analysis of Variance (ANOVA) for the three selected materials and their variations with ultrasonic frequencies and infrared powers
4. To analyse the data using the existing of theoretical model of dependence of effective diffusion coefficients on the slice thicknesses and validated.

1.5 Organization of the Thesis

This thesis contains of six chapters as shown following:

Chapter 1 (Introduction) introduces the different drying processes and the principal mechanisms of the drying including the roles of effective diffusion coefficients, particularly in drying of slices of materials. This chapter also presented the scope of study as well as problem statement and objectives of the study.

Chapter 2 (Literature review) describes the theory of moisture transfer and influence of parameters in the convective drying. The theory of effective diffusion coefficients and effect of slice thickness on effective diffusion coefficients is described. The various types of models of sliced materials are presented. The theory and previous studies of analysis of Arrhenius constants and activation energies is also described. This chapter also describes theory and mechanism of ultrasonic energy or infrared radiation as well as presents the previous studies of ultrasonic or infrared application as well as effect of ultrasonic frequency or infrared power in drying rates and effective diffusion coefficients of drying process. The theory and mechanism of combined ultrasonic and infrared application is also discussed in this chapter. This

chapter also describes the theory of Design of Experiment (DOE) including central composite design (CCD), response surface methodology (RSM) and Analysis of Variance (ANOVA).

Chapter 3 (Materials and methods) describes the detail of the materials selected, equipment used, experimental procedures and procedures used in data analysis. The detail of DOE also has been described in this chapter. The overall flow chart for this study is presented.

Chapter 4 (Modelling studies) describes the theoretical model developed in this study for estimation of axial and radial diffusion coefficients from effective diffusion coefficients and also details of statistical modelling. The steps of model formulated of dependence of effective diffusion coefficient on slice thickness are included in this chapter. The method of statistical analysis (ANOVA) of effective diffusion coefficient, axial and radial diffusion coefficient, Arrhenius constant and activation energy is also described in this chapter.

Chapter 5 (Results and discussions) presents the results obtained from experiments which are moisture ratios and results evaluated which are effective diffusion coefficients, axial and radial diffusion coefficients, Arrhenius constants and activation energies. The variation of the respective diffusion coefficients with the parameters namely ultrasonic frequency and infrared power for different air temperatures were evaluated and discussed in this chapter.

Chapter 6 (Conclusion and recommendation) concludes the finding of the study and recommendation for the improvement in future research.

CHAPTER 2

LITERATURE REVIEW

2.1 Convective Drying

2.1.1 Convective drying process

Convective drying has been a conventional method used to carry out the drying process of the agricultural products. In convective drying process, hot air is passed over the samples to be dried in a chamber where the moisture is removed from wet materials (Noomhorm, 2007). Two simultaneous processes occur during the convective drying of materials. These are (a) heat transfer from the hot air to the wet material to be dried and (b) moisture diffusion from the internal of the wet material to the surface as a result of evaporation of moisture from outer layer of the wet material which generate a concentration gradient of moisture within the material (McMinn and Magee, 1999).

2.1.2 Theory of moisture transfer in convective drying

The important properties which determine the drying process of the moisture in the materials have been found to be the amount of the moisture present in the materials and the state of the moisture molecules, i.e. whether the moisture is free or bound (McMinn and Magee, 1999). Here, moisture within wet materials has been categorized as free moisture (mechanically or physicochemically) and bound moisture (chemically bonded) attached to the materials (McMinn and Magee, 1999). The free moisture has been found to locate in the interstitial spaces and pores of the material by physical forces such as surface tension or van der Waals forces. The properties of free moisture are similar to those of pure water. The bound moisture has

been the moisture attached to the solid by chemical bonding. The bound moisture exists as monolayer or multi-layer with moisture-moisture bond or solid-moisture bond on the internal or external surface of the materials (McMinn and Magee, 1999). The kinetic and thermodynamic properties of bound moisture are very different with the pure water (Noomhorm, 2007).

As discussed in Section 1.1.3, the two primary regions of drying are existed namely the constant rate and the falling rate. The drying of many agricultural products is fall within the falling rate (Swami *et al.*, 2007; Doymaz, 2007; Doymaz and Gol, 2009; Sojak and Glowacki, 2010). The falling rate has been reported to be the moisture transfer from the interior to the outer surface of the materials (McMinn and Magee, 1999; Puyate and Lawrence, 2006). The moisture transfer process is also known as the moisture diffusion process (Seader and Henley, 1998). The moisture diffusion process (Fick's second law of diffusion) is presented in detail in Section 2.2. The drying rates of many agricultural products can be enhanced by employing sliced samples (Aysun *et al.*, 2002; Mwithiga and Olwal, 2005; Rao *et al.*, 2007; Doymaz and Gol, 2009). This study concentrates on drying and diffusion of sliced samples.

2.1.3 Parameters influencing rates in convective drying

Several studies (Sharma and Prasad, 2001; Aysun *et al.*, 2002; Mwithiga and Olwal, 2005; Doymaz, 2007; Nguyen and Price, 2007) have been carried out to investigate the phenomena involved in the convective drying process of slices. These studies have attempted to predict the drying rate and study the influence of the processing variables on the drying rate. The process variables such as air velocity, air

temperature and sliced thickness which govern the drying rates are discussed in detail in the following sections.

2.1.3.1 Air velocity

Sharma and Prasad (2001) have studied the hot air drying of 15 g of garlic cloves at air velocities of 1 m/s and 2 m/s and air temperatures of 50°C to 70°C. It was observed that enhancement of the drying time resulted when air velocities were increased from 1.0 m/s to 2.0 m/s. This was attributed to the increased in heat absorbed by the sample due to higher heat transfer coefficients at higher air velocities. Aysun *et al.* (2002) have studied the hot air drying of grape leather at air velocities of 0.86 m/s, 1.27 m/s and 1.82 m/s of at air temperature of 75°C and slice thickness of 2.2 mm. The results showed that the drying time decreased when the air velocities increased from 0.86 m/s to 1.82 m/s and this result indicated that higher drying rates at high air velocities. Swami *et al.* (2007) have studied the convective drying of bori with dimension of 20-38 mm in diameter and 10-23 mm in height at air temperature of 30°C to 70°C and air velocity of 0.6 m/s to 1.4 m/s respectively. A statistical analysis (ANOVA) has been carried out by them thereafter and a second order polynomial equation for drying time, t (s) with temperature, T (K) and air velocity, v (m/s) as shown in Equation (2.1) has been obtained. The model has been validated with the experimental data satisfactory with a correlation coefficient ($R^2 = 0.95$). This model indicated that a dependence of drying time on the air velocity and air temperature.

$$t = 209.61 - 183.21T - 163.05v + 85.88T^2 + 171.94Tv + 104.59v^2 \quad (2.1)$$

2.1.3.2 Air temperature

Doymaz (2007) has studied the moisture ratio (ratio of the moisture content at time, t to the initial moisture content) of 0.7 cm of pumpkin slices for drying at air temperatures of 50°C, 55°C and 60°C and 1 m/s of air velocity respectively. He found that the drying times were 750 minutes, 390 minutes and 270 minutes respectively for the drying of pumpkin slices from the initial moisture content of $92.4 \pm 0.2\%$ to a final moisture content of $10 \pm 0.3\%$. The results have shown that drying time decreased rapidly with increased in temperature. This was attributed to higher heat transfer in the drying process at high temperatures. Nguyen and Price (2007) also have shown that the drying time decreased when air temperature increased for convective drying process. The convective drying process at air velocity of 1 m/s and banana slices of 1 cm to obtain 70% mass loss in banana has shown that the drying time decreased from 2100 minutes to 660 minutes when the air temperature increased from 30°C to 70°C. Rao *et al.* (2007) have studied the convective drying process of paddy at air temperature of 70°C to 150°C and air velocity of 0.5 m/s to 2.0 m/s with grain bed depth of 5 cm to 20 cm. A second order polynomial equation for drying time, t (min) with grain bed depth, ℓ (m), air temperature, T (K) and air velocity, v (m/s) has been obtained by statistical analysis (ANOVA) with a correlation coefficient ($R^2 = 0.98$).

$$t = 216.57 + 8.57\ell - 2.14T - 105.08v - 0.07\ell^2 + 0.005T^2 + 0.44Tv - 1.44\ell v - 0.02\ell T + 18.50v^2 \quad (2.2)$$

In general, the drying rate was observed increased at high air temperatures.

2.1.3.3 Sliced thickness

Aysun *et al.* (2002) have studied the hot air drying of grape leather slices at 0.71 mm, 1.53 mm, 2.20 mm and 2.86 mm at air temperature of 75°C and air velocity of 1.75 m/s. The drying time was observed increased from 40 minutes to 140 minutes when the slice thickness increased from 0.71 mm to 2.86 mm. Mwithiga and Olwal (2005) have studied the effect of the thickness of sample on the drying time for hot air drying of kale at air temperature of 60°C and air velocity of 1 m/s. The drying time for kale increased from 340 minutes to 1300 minutes when the thickness of sample increased from 10 mm to 50 mm. The results have shown that the drying times increased with increased of thickness of sample. Doymaz and Gol, (2009) have studied the drying of 0.5 cm to 1 cm of eggplant slices at air temperature of 50°C to 80°C and air velocity of 2 m/s. The drying time was observed increased from 240 minutes to 290 minutes with increased of slice thickness from 0.5 cm to 1 cm. It has been explained as easier of moisture transfer due to short distances for moisture transfer in thin slices which led to decrease the drying time for the thin slices. Rao *et al.* (2007) have studied the drying of paddy with grain bed depth of 5 cm to 20 cm at air temperature of 70°C to 150°C and air velocity of 0.5 m/s to 2.0 m/s. They developed a second order polynomial statistical model for drying time, t (min) with grain bed depth, ℓ (m), air temperature, T (K) and air velocity, v (m/s) with a correlation coefficient ($R^2 = 0.98$) as shown in Equation (2.2). It was observed from the model that the drying time is dependent on the grain bed depth where drying time increased with increased of grain bed depth.

2.2 Diffusion Process in Convective Drying

2.2.1 Effective diffusion coefficients

In drying processes, the possible mechanisms of moisture transfer within materials included diffusion of moisture caused by its concentration gradients within materials, moisture transport caused by capillary forces and gravity, vapour diffusion due to shrinkage and partial vapour-pressure gradients, moisture or vapour transport due to the difference in total pressure caused by external variations of pressure and temperature, evaporation and condensation effects caused by differences in temperature and surface diffusion in moisture layers at the solid interface due to surface concentration gradient (Gavrila *et al.*, 2008). Most of the materials in drying process have been classified as capillary porous rigid or capillary porous colloids materials (Gavrila *et al.*, 2008). Capillary flow has been accepted as one of the mechanisms of the moisture transfer especially at high moisture contents (McMinn and Magee, 1999). A combination of capillary flow and moisture diffusion mechanisms has been shown to satisfactorily describe the internal moisture transfer within the drying materials. However, the moisture diffusion theory described by Fick's second law of diffusion has been commonly accepted as the primary theory and governing drying has been widely used by many researchers in drying processes of agricultural products (Jorge *et al.*, 2002; Puyate and Lawrence, 2006).

Hence, it has been commonly accepted that moisture diffusion mechanism primarily controlled the drying mechanism of the agricultural products particularly during the falling rate period (McMinn and Magee, 1999; Akpinar, 2006). Models for drying of slices and thin layers commonly known as thin layer models which have been used to describe the drying rate of agricultural products (Aleksandra, 2007)